

We are IntechOpen, the world's leading publisher of Open Access books Built by scientists, for scientists

6,900

Open access books available

185,000

International authors and editors

200M

Downloads

Our authors are among the

154

Countries delivered to

TOP 1%

most cited scientists

12.2%

Contributors from top 500 universities



WEB OF SCIENCE™

Selection of our books indexed in the Book Citation Index
in Web of Science™ Core Collection (BKCI)

Interested in publishing with us?
Contact book.department@intechopen.com

Numbers displayed above are based on latest data collected.
For more information visit www.intechopen.com



Using of Magnetron Sputtering for Biocompatible Composites Creating

Elena O. Nasakina, Mikhail A. Sevostyanov, Alexander S. Baikin, Sergey V. Konushkin, Konstantin V. Sergienko, Mikhail A. Kaplan, Ilya M. Fedjuk, Alexander V. Leonov and Alexey G. Kolmakov

Abstract

Biocompatible composites obtained using the magnetron sputtering for the production of minimally invasive implantation medical devices (stents) were investigated. Nano- and microdimensional surface layers of Ta, Ti, Ag, and Cu on flat and wire NiTi, Cu, Ti, and SiO₂ substrates were created. The phase composition, surface morphology, and the layer-by-layer composition were investigated on an X-ray diffractometer, SEM, and Auger spectrometer. It was shown that the thickness and the structure of surface layers were affected by the sputtering distance, time, power, and the bias voltage at the substrate. The presence of the transition layer that contains both substrate and target elements and provides high adhesion of the surface layer to the substrate has been demonstrated. The material was tested for corrosion resistance under static conditions by dipping into solutions with various acidities (pH from 1.68 to 9.18) for 2 years, static mechanical properties, and biocompatibility in vitro and in vivo. A slight corrosive dissolution was observed only in a medium with a pH of 1.56. Dissolution in the other media is absent. An increase in strength and plasticity in comparison with substrate was attained depending on the nature of the sputtered substance and substrate. Toxicity of samples has not been revealed.

Keywords: surface layer, magnetron sputtering, biocompatibility, corrosion resistance, shape memory effect and pseudoelasticity

1. Introduction

In the modern world, an efficient manner of operational characteristic increase and of classical material shortcoming elimination is a formation on their basis of composite materials [1–6]. Development of the layered composite materials allowing to effectively combine desirable operational characteristics of the modified surface layers and the main material (substrate) at the present time is perspective in many areas of human activity: in optics (conducting, antireflecting, filtering, reflecting, and

absorbing media), electronics (conductors, semiconductors, dielectrics), machine engineering, building and household (tribological, durable, wear-resistant, functional, protective, resistant to action of aggressive environment, decorative, and other coatings for structural and utility materials), medicine (biocompatible materials), etc. [1–17].

An effective and fairly common method for such surfaces formation is physical vapor deposition, including variations of magnetron sputtering, since at relatively small expenditure of time and resources, it allows to efficiently receive qualitative thin films of a diverse nature on substrate of virtually any nature and geometry and to control properties of the created materials [7–17]. The deposition method developed at the Baikov Institute of Metallurgy and Materials Science allows one to produce [coating—transition layer—substrate] nanocompositions from thermodynamically nonmiscible elements with good adhesion and resistance to external thermal and mechanical influences [18] and at the same time to avoid substrate overheating with bombarding electrons by keeping them near the sputtering target, which is of high importance for substrate materials with low melting points or phase structure that is sensitive to temperature changes [7].

Among other things, this technology can be successfully used in the formation of medical composite materials that need to have complex properties, combining only the required characteristics of classical materials—for example, for the production of noninvasive stent implants designed to restore the patency of hollow parts of the cardiovascular, excretory, digestive, and respiratory systems [19, 20]. At the same time, the parameters of the resulting composites depend on a number of process conditions that can be conveniently varied over a wide range.

In addition, the initial choice of the components of the future composite is important. Materials with the shape memory effect are the best candidates for creation of medical implants plastically deformable in the cooled condition to extremely compact type promoting easier and less traumatic delivery to the necessary site of an organism without serious surgical intervention. Then, they independently take the functional form in set operational conditions without additional effect [20–23]. The most known medical material from this class is nitinol (NiTi) endowed with mechanical characteristics similar to behavior of living tissues that helps it to adapt to physiological loadings providing necessary service conditions [20–23]. But in addition to positive mechanical characteristics, this alloy possesses also a number of shortcomings: difficulty of processing in case of product production, the high content of a toxic element, disputable level of biocompatibility, and corrosion resistance. Research toward its improvement is actively conducted [23–25]. Thus, nitinol can be taken as the basis of the composite (substrate) and a biologically inert barrier at the contact between the metallic parts of the implant and active biological body fluids is needed. A new surface should be represented by a material with high corrosion resistance and biocompatibility. For example, tantalum and titanium is interesting due to high corrosion resistance in aggressive media, radiopacity, conductivity, wear resistance, nontoxicity, etc. [6]. Silver also exhibiting antitumor and antibacterial action is one of the suitable materials [26].

The purpose of this work was to investigate capabilities and regularities of production of layered biomedical composite materials based on an NiTi shape memory alloy with a surface layer from highly corrosion-resistant and biocompatible tantalum, titanium, or silver with strong adhesion between the components formed by magnetron sputtering and to study its operational properties.

2. Obtaining and investigating of biocompatible composites of medical appointment

In this work, creation of layered composites was carried out by formation of tantalum, titanium, silver, etc., surface layers on flat and wire nitinol, titanium, glass/SiO₂, etc., substrates (basis) by magnetron sputtering in an argon atmosphere by using a Torr International facility (United States). Working and residual pressure in the vacuum chamber was 0.4 and 4×10^{-4} Pa, respectively.

The surface layers were produced under the following conditions of the process: (1) direct current magnetron, in the case of tantalum and titanium layers $I \sim 400\text{--}1100$ mA, $U \sim 360\text{--}700$ V; in the case of silver layers $I \approx 865$ mA, $U \sim 830$ V; (2) with substrate rotation (rate was 9 rpm) and without it; (3) sputtering time $t = 5$ to 120 min; (4) bias voltage $U_b \approx 0\text{--}1000$ V; and (5) sputtering distance (the distance from the target to the substrate) of 40–200 mm.

To avoid overheating, the substrate is critically important for substrate materials with phase structures that are sensitive to temperature changes as nitinol, for example—the thermal treatment allows one to vary static properties and cyclic loadings in operating conditions with a wide range of deformations and is extremely important for stabilization of the properties, constraining (shaping) the samples, and successful application of the product.

To determine the substrate surface temperature, we used special control samples from materials with various melting points: In ($t_m = 156.4^\circ\text{C}$), Sn ($t_m = 231.9^\circ\text{C}$), Pb ($t_m = 327.4^\circ\text{C}$), and Zn ($t_m = 419.5^\circ\text{C}$). Since none of the metals showed surface melting, we concluded that, under any conditions, the substrate surface temperature did not reach 150°C in any of the regimes used.

Disks made from chemically pure tantalum, titanium, silver, copper, etc., were used as the sputtered target. Plates made from nitinol, titanium, copper, steel, glass/SiO₂, etc., with a size of $10 \times 10 \times 0.5$ mm and 280 μm diameter wires from nanostructured nitinol (with the composition 55.91 wt% Ni + 44.03 wt% Ti, having grains in the form of 30 to 70 nm diameter nanowires and a cubic crystal lattice (B2 phase)) were used as the basis for composites. Plates were treated with abrasive sandpaper (from 400 to 800 grit) and polished (until their surface became mirror-like) with the addition of diamond suspensions with a particle size of 3, 1, and 0.05 μm for the removal of flat indentations and defects. Nitinol wires were also polished consecutively with sandpaper from 180 to 1000 grit and subjected to finishing polishing with GOI (State Optical Institute) paste to a mirror surface. The decrease in the diameter was to 10 μm in comparison with the original. The depth of surface defects after the processing was less than 1 μm . Different substrates were selected to perfect the production of layered composites. Silicon, copper, and steel substrates are also of interest as a basis for production of functional materials for a wide range of applications (optics, electronics, construction materials, etc.). To clean, activate, and polish the substrate surface, before sputtering, it was bombarded with argon ions at $U_e = 900$ V and $I_e = 80$ mA; i.e., preliminary ionic etching (PIE) was performed.

Phase structure of the deposited films was characterized by the Ultima IV X-ray diffractometer (Rigaku Co., Japan) in Cu K α —radiation on the base of Bragg—Brentano method. Phase analysis was prepared in the PDXL program complex using the ICDD database. The surface morphology and the layer-by-layer composition were investigated on a scanning electron microscope (SEM) VEGA II SBU with the module INCA Energy for energy-dispersive analysis (TESCAN, Czech Republic), on a GDS 850A atomic emission spectrometer (JEOL Co., Japan), and on a JAMP-9500F Auger spectrometer (JEOL Co., Japan) in combination with ion etching at argon bombardment under an angle of 30° . In Auger electron spectroscopy,

the surface layer thickness was taken to be equal to the depth at which the atomic percentages of the constituent elements plateaued. Fracture surfaces were also examined on the TESCAN VEGA II SBU.

On the whole, similar results were obtained by examining the surface layer composition (**Figure 1**): the top surface layer was oxygen-enriched to a depth of 20 nm owing to active surface adsorption, a deeper layer consisted of only submitted element, and the transition layer was also oxygen enriched and resided on the substrate. The formation of the transition layer is connected with the fact that magnetron sputtering results in atoms and ions of the sputtered substance not only condensing on the substrate surface but also approaching it with some excess energy with their contact leading to a number of interparticle interactions: “knocking in” of sputtered atoms and ions, “knocking out” by them (upon elastic or inelastic interaction with or without transfer of their additional energy), and redeposition or, on the contrary, penetration of the surface particles (both of the substrate and earlier deposited elements) into the substrate structure, formation of radiation defects that stimulate mutual diffusion of elements of the deposited layer and substrate at their interface, etc. Thus, the mobilized particles, sputtered substance, and surface region of the substrate that are subjected to multiple collisions and set in chaotic motion at or near the substrate surface are constantly mixed. In the end, the surface region becomes so saturated by the sputtered substance that its interaction with new flows of atoms and ions leads to the formation of the surface layer of the composite.

Figure 2a shows dependence of tantalum surface layer thickness from time of magnetron sputtering on a nitinol substrate. Increasing the sputtering time to 20 min (at direct current of 865 mA, voltage of 700 V and distance 200 mm) increased the thickness of both the surface layer (consisting only of the deposited substance) and the transition layer (containing elements of both the substrate and deposited substance). Further increasing the sputtering time caused an increase only in the thickness of the surface layer, which varied nonlinearly, following a descending law, and up to 30 min more intensively, than at bigger time. This situation remains at all used materials and conditions. It occurs, most likely, because at the beginning of surface layer formation, atoms and ions of deposited substance, overcoming a sputtering distance, collide with particles of working gas, with each other and with new substrate surface and do not appear at each site of its surface in equal volume and at the beginning interact with it chaotically and unevenly. And further (at increase of sputtering time, and so of the time of influence on a surface), particles continue to collide, mixing up, try to reach thermodynamically more advantageous position and state, and a more uniform distribution of the deposited substance at the surfaces takes place. By consideration of cross section of samples, it

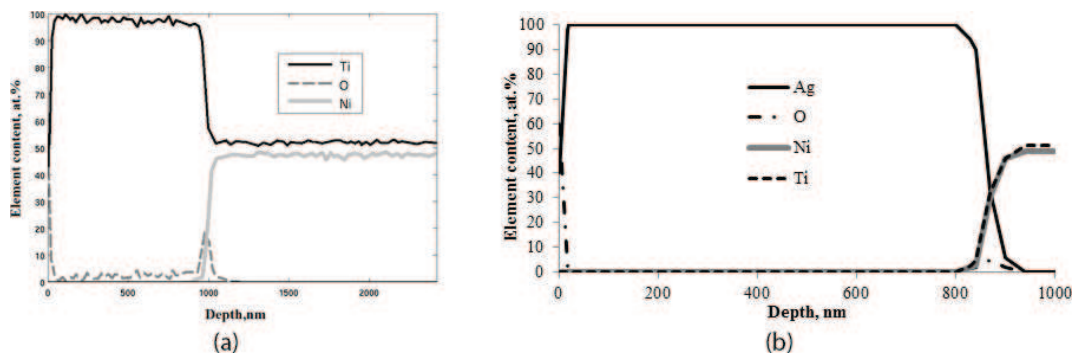


Figure 1. Composition depth profiles for a Ti-nitinol sample obtained by sputtering for 30 min at direct current of 865 mA, voltage of 700 V, and distance of 200 mm (a) and for Ag-nitinol obtained at a distance of 150 mm (b).

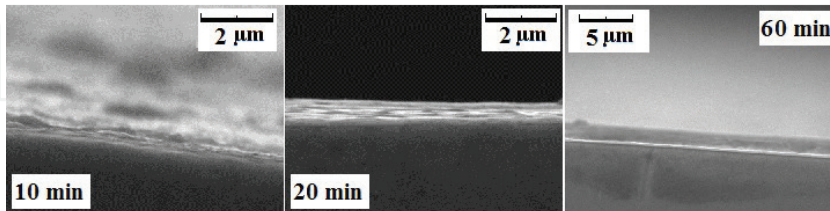
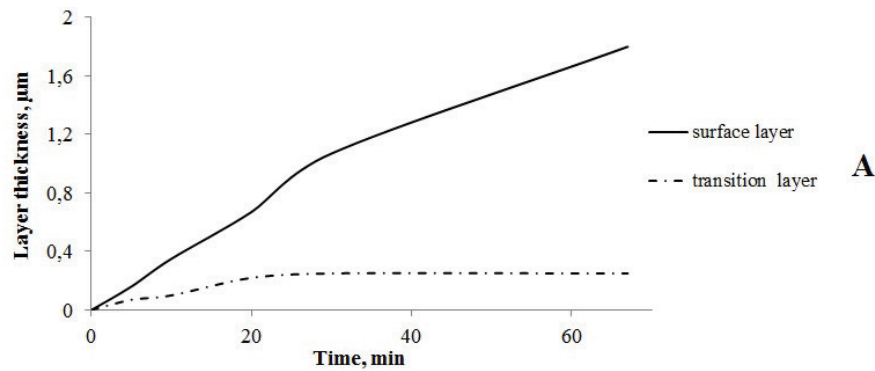


Figure 2. Dependence of the surface layer structure on the time of magnetron sputtering of tantalum on a nitinol substrate at direct current of 865 mA, voltage of 700 V, and distance 200 mm (a) and microstructure changes (b).

is visible that at smaller time of a sputtering, the surface shows a big heterogeneity (**Figure 2b**). First, the layer had the form of isolated islands. Subsequently, a more uniform Ta distribution over the substrate surface was obtained.

In case of thin films of tantalum, according to literary data, formation of both alpha and beta phases, which differ in properties, is possible [10–17, 27–29]. The X-ray diffraction patterns of our samples with nitinol basis (**Figure 3**) demonstrate that depending on sputtering, time tantalum is formed in two various crystal states—an alpha (a cubic crystal lattice) and a beta (a tetragonal lattice with the small content of oxygen).

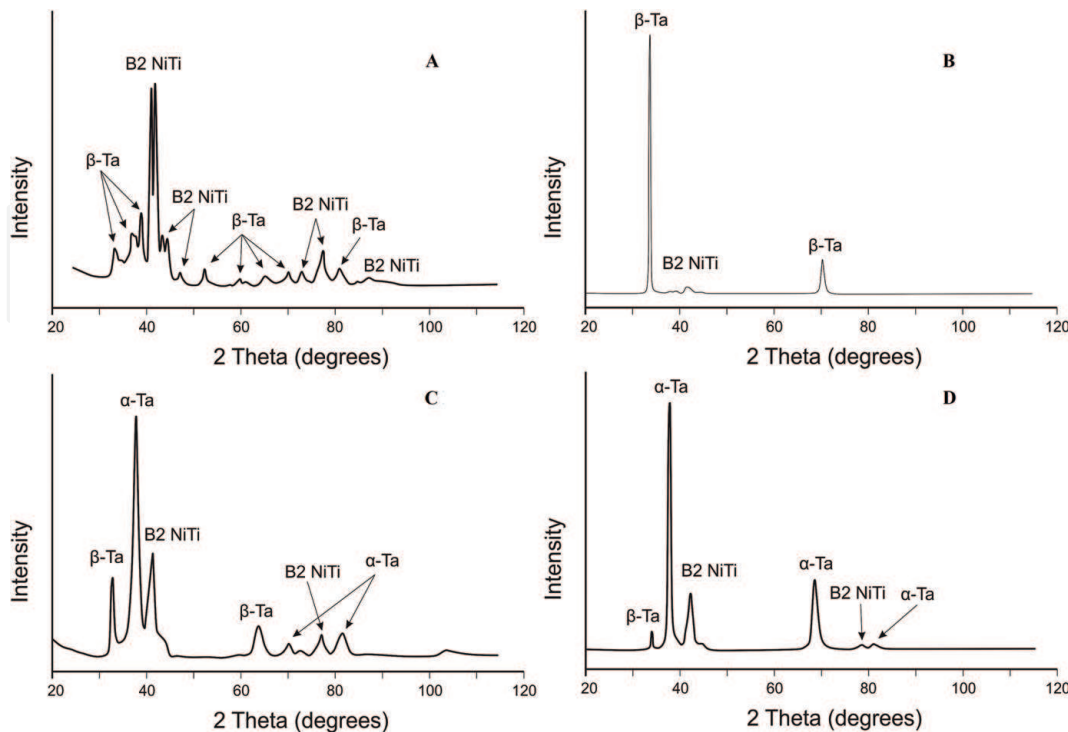


Figure 3. X-ray diffraction patterns of a composite on the basis of a nitinol received at magnetron sputtering time: (a) 5 min, (b) 10 and 20 min, (c) 29 min, (d) 30 min at direct current of 865 mA, voltage of 700 V and distance of 200 mm.

In the case of a sample with a Ta surface layer obtained by sputtering for 5 min, the major phase was nitinol, but many peaks β -Ta in the 2-theta range from 33 to 81° were observed, which also corresponds to various crystal orientation. In the composites formed after sputtering for 10 and 20 min, β -Ta with O were a major phase, and only two main peaks were observed, but nitinol was also present. After 29 min, the strongest peak was that from α -Ta, and there were β -Ta with O and nitinol, due to the averaging of results over the entire probing depth; at further increase in time, α -Ta dominated and very weak peaks of β -Ta and nitinol were observed. Thus, it turns out that irrespective of summary sputtering time, the beta phase is formed in the beginning and at sputtering time, more than 20 min on it, alpha tantalum is deposited. The same regularities are observed in case of other substrates, which are united by availability of oxygen in a surface. In contrast to data available in the literature, the formation of α -Ta in this study cannot be due to an increase in temperature [10, 14, 27, 28].

Several theories of tantalum formation in α or β phase is developed, which are generally connected with working temperature and pressure (defining mobility and energy of atoms) and the substrate nature. However, different authors achieve often contradictory results.

It is noted that the alpha phase is formed at temperatures more than 400°C, promoting mobility increase in deposited atoms: initially at heating of a substrate or as a result of the annealing following sedimentation (then deposited β -Ta transforms in α -Ta) [10, 14, 27, 28]. However at a temperature about 400–500°C, β phase is also received (for example, in the form of the particles distributed in α) [10, 28], and α is also formed without heating [12, 15]. It is specified that with the growth of temperature, the size of grains, impurity amount in a surface layer (for example, the dissociation of oxides enhanced, i.e., the O contents lowered), and its amorphousness decreases.

Presence at the working atmosphere of the high oxygen content according to [16] leads to fast formation of oxides and, therefore, promotes formation of a tantalum layer in a beta state, whereas in [15], oxygen environment did not prevent the formation of alpha tantalum. At a deposition on silicon and glass substrates in [13, 16, 17], 0.5–0.7 Pa sputtering pressure led to α -Ta formation and smaller or bigger pressure— β -Ta, but in [15] already at 0.28 Pa, α phase was formed.

In [17], alpha tantalum was also formed at 0.3 and 1.4 Pa pressure, but at sputtering on earlier deposited α -Ta (110) layer. Also, it was specified that (110) is the most low-energy lattice for body-centered cubic (BCC) materials and provokes formation on itself of the same structure. Being a zone of a new surface nucleation, the substrate surface specifies the character of its structure formation. It was shown that on amorphous carboniferous or oxidic surfaces, the beta tantalum is formed, for example, on titanium without natural oxide or TaN substrates, the α -Ta is formed [11, 12, 14, 17].

And though availability of oxygen on a substrate surface not always prevented the formation of α -Ta, nevertheless, it is considered that it promotes formation of β -Ta. Therefore, its creation in this work in an initial time period on all substrates is quite expected, despite ionic etching.

In [14], as well as in this research, it was shown that longer time promotes layering of α -Ta on earlier formed β -Ta, but authors connected it with a considerable warming up of a surface (more than 350°C), whereas in this work, temperature of a substrate did not rise higher than 150°C and so could not influence formation of alpha phase. It is worth noting that α -Ta is a more thermodynamically stable phase. It is, therefore, reasonable to assume that, in this study, it results from a more uniform surface coverage with increasing sputtering time (because increasing the sputtering time increases the probability that a particle will find a more appropriate state and position), possible local surface heating (within several atomic layers,

which cannot be detected visually), and the absence of oxygen (incorporated into the β -Ta sublayer) [11, 12, 14, 17].

In combination with the above results of layer composition, this X-ray diffraction data lead us to assume that the surfaces of both the substrate and surface layer actively adsorbed oxygen and that, in the initial stage of the process, the sputtering time was too short for a purely metallic tantalum layer to form.

Purely silver or titanium layers in a single phase are formed on nitinol at all conditions, which is reflected in an X-ray pattern by characteristic peaks (**Figure 4**) [26].

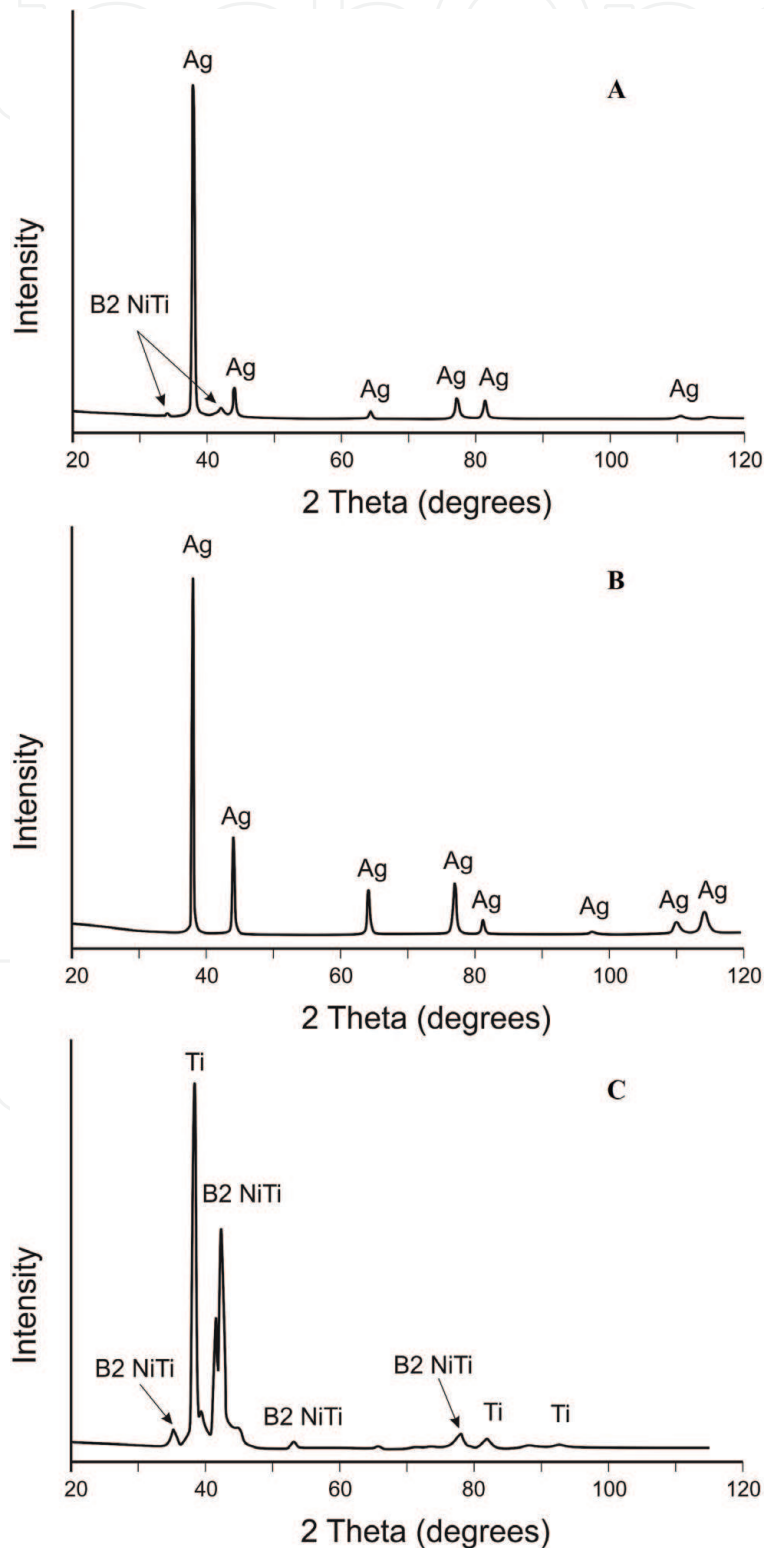


Figure 4. X-ray patterns of Ag-NiTi composites obtained by sputtering: (a) for 20 min, (b) for 30 min, and (c) Ti-NiTi for 30 min at a distance of 150 mm, 865 mA, and 400 V.

A composite with silver that is produced for 30 min has only Ag peaks observed because of natural growth of the thickness of the surface layer. At a sputtering time of 20 min or in Ti-NiTi composite produced for 20 and 30 min, the main phase is a sputtered metal, but also traces of the nitinol substrate are observed owing to data averaging over the depth. These results are repeated with all the used substrates.

Figure 5 shows the dependence of the thickness of the surface tantalum layer (produced for 30 min at ~ 865 mA, ~ 700 V, a sputtering distance of 200 mm and with PIE on a flat nitinol substrate) on the applied negative bias voltage that was instrumental in the process of ion-atomic deposition [7, 18]. The bias voltage affected both the thickness and the structure of layers: a voltage of 100 V reduced (relative to zero voltage bias) the thickness of the surface and the complete layers supposedly because of the structure densification by the additional ionic bombardment. At higher voltages, the surface layer became thicker owing to an increase in the rate of deposition of the sputtered material, while the thickness of the transition layer was reduced somewhat (apparently because of further densification of its structure). The optimum conditions were attained at 500 V, and the further increase in the bias voltage probably led to certain sputtering of the surface: the thickness of the surface layer was reduced again, while the thickness of the transition layer remained the same.

Large corrugations with a length on the order of 20–10 μm and a width of 3–5 μm were observed at the surface of all samples (**Figure 6**). Their characteristic appearance did not change with applied bias voltage, and they did not disappear after a layer with a thickness of about 10 nm was etched out. Therefore, they may be interpreted as the initial microrelief of the sample surface. When the bias voltage was applied, smaller wavelike corrugations with a length of 6–10 μm and a width of 0.5–1 μm emerged at the surfaces of samples. An increase in the bias voltage from 100 to 1000 V led to the gradual smoothing of these corrugations, which were easily observable at first, but became virtually imperceptible at 1000 V. The surface after 1000 V did not differ from the one obtained under zero voltage bias (**Figure 6**). The emergence of smaller scale corrugations may probably be attributed to the presence of residual compressive stresses at the composite surface. A bias voltage of 500 V triggered a uniform distribution of point dimples that likely represented the traces of ion bombardment [9], but these pits and all other inhomogeneities of a similar scale disappeared after a layer with a thickness of about 10 nm was etched out.

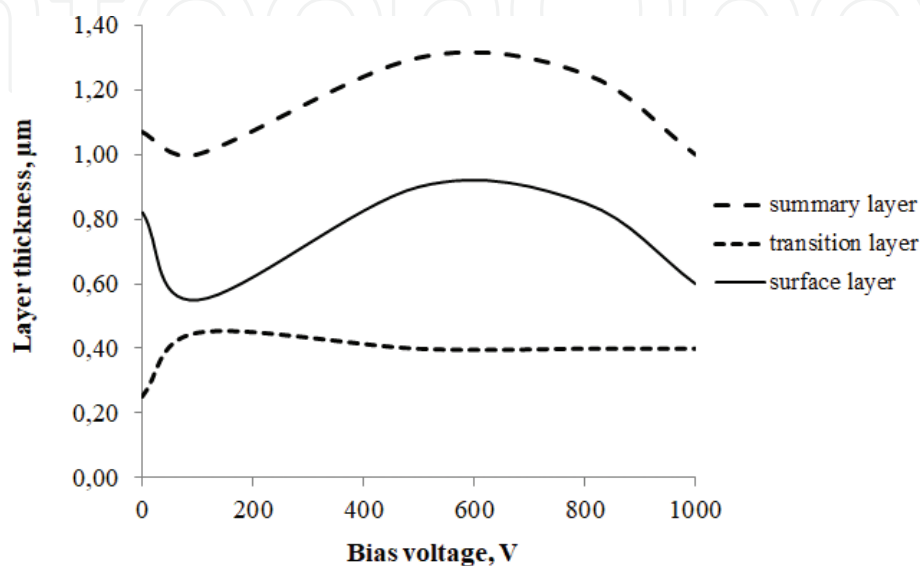


Figure 5. Dependence of the thickness of the surface tantalum layer produced on a nitinol substrate at ~ 865 mA, ~ 700 V, a sputtering distance of 20 cm, and with PIE for 30 min on the bias voltage.

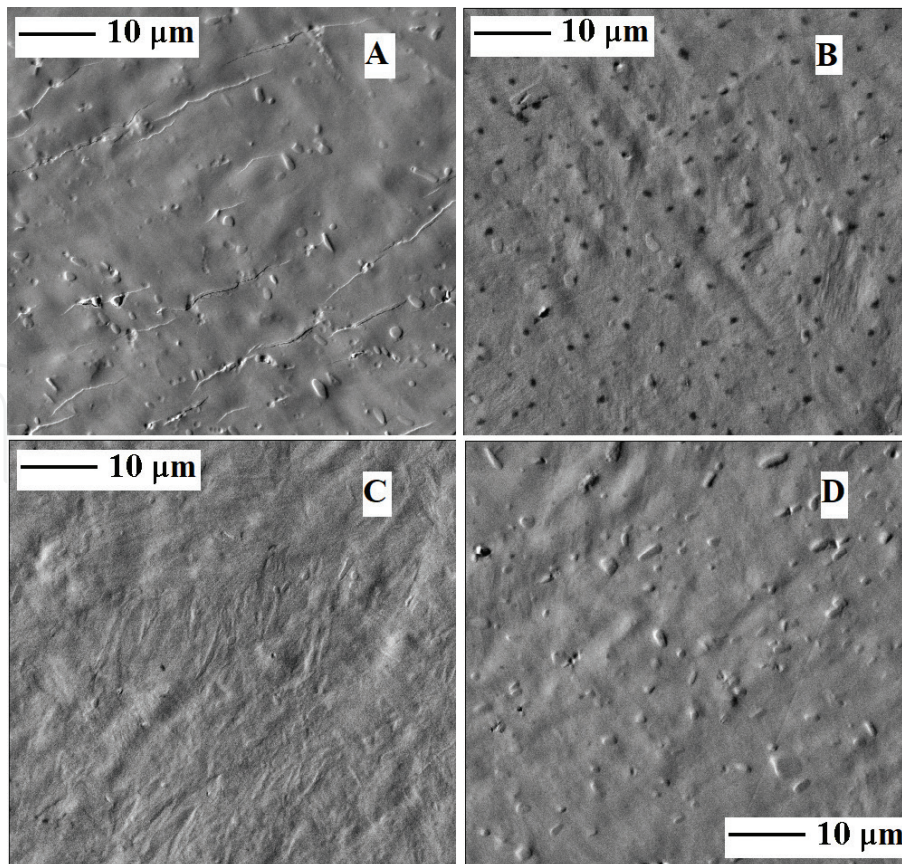


Figure 6. Appearance of the surface tantalum layer produced on a titanium nickelide substrate at ~ 865 mA, ~ 700 V, and a sputtering distance of 15 cm (the sputtering process took 30 min) under $U_b =$ (a) 100, (b) 500, (c) 800, and (d) 1000 V.

The overall thickness of surface layers was increased almost linearly with sputtering power. The thicknesses of both the surface and the transition layers were raised to 30% of the maximum value (**Figure 7**). The thickness of the transition layer was reduced in the 30–50% power interval, while both the surface and the transition layers became thicker again at higher powers. The increase in their thicknesses may be attributed to the raised target sputtering rate [7], and the temporary reduction in the transition layers thickness may be associated with the structure

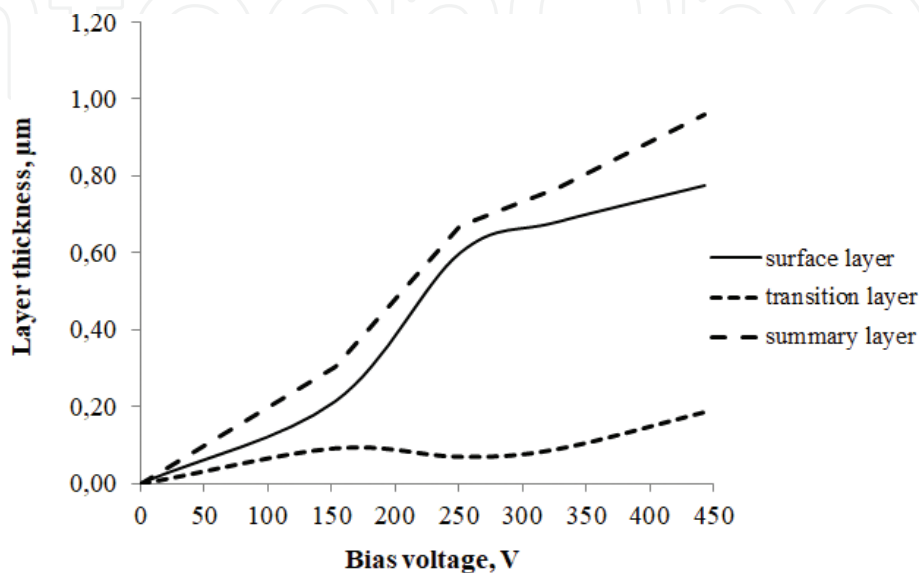


Figure 7. Dependence of the thickness of the surface titanium layer produced on a glass substrate at ~ 865 mA, ~ 400 V, a sputtering distance of 150 mm, $U_b \sim 0$ V, for 30 min on the sputtering power.

densification and a reduction in the available formation time with increasing energy and density of the flux of sputtered material. When the tantalum sputtering power was raised above 70%, the thickness of the surface layer increased only slightly, and the thickness of the transition layer remained the same (on a metal substrate) or was increased (on a glass substrate; see **Figure 7**) presumably owing to the influence of pores in the material. This also raised the target consumption rate and the potential to contaminate the surface of the composite with, among other things, elements of the walls of the working chamber that are knocked out by high energy particles.

On the one hand, with distance increasing at other equal conditions, the thickness of the tantalum surface layer naturally decreases (**Figure 8**) because larger volume of the sputtered substance is scattered away from the substrate; on the other hand, the thickness of the transition layer increases, which can be explained by a more intense flow of the sputtered substance at a shorter distance, uniformly but faster filling the surface and less diffusing into the substrate; and the total thickness of the layers eventually reaches a certain plateau, practically unchanged when the distance is more than 80–90 mm. Since the presence of a substantial transition layer is a presumable reason for the good adhesion of a new surface to the substrate [6], the surface layer must be adjusted to the mechanical properties of the substrate, and also considering the microdefects of the surface at small distances, the distances from the target to the substrate in the range of 100–150 mm are more optimum.

In contrast to tantalum, where the appearance of the surface layer thickness curve completely corresponds to the calculated models [7], in the case of a silver layer, two plateaus are observed (**Figure 9**): almost constant thicknesses at small sputtering distances can be attributed to saturation of the surface at high intensities of flux falling on the substrate. Unlike the previous case, both the surface layer and the transition layer are thinned with increasing distance, because a smaller volume of substance reached its goal, but the intensity of the flow did not affect the formation of the transition layer.

Visually, the layer thickness also was reduced (**Figure 10**) as the sputtering distance was increased under otherwise equal conditions. At smaller distances from the target to the substrate, no appreciable transition layer was observed in SEM images.

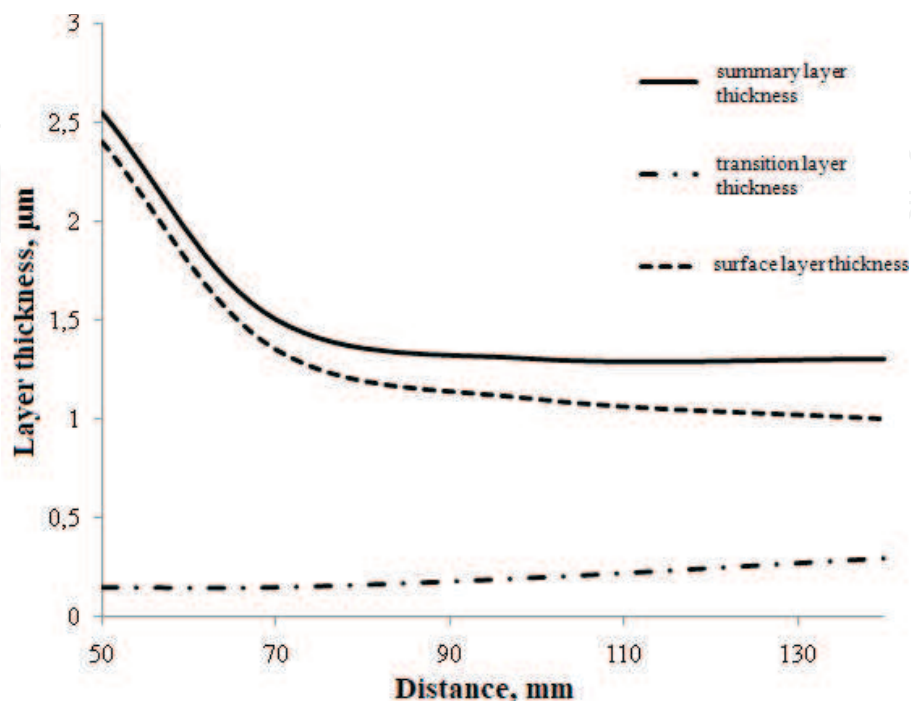


Figure 8.

Change in the tantalum surface layers thickness as a function of the distance between the target and the substrate for composite obtained for 30 min at 400 V, 865 mA.

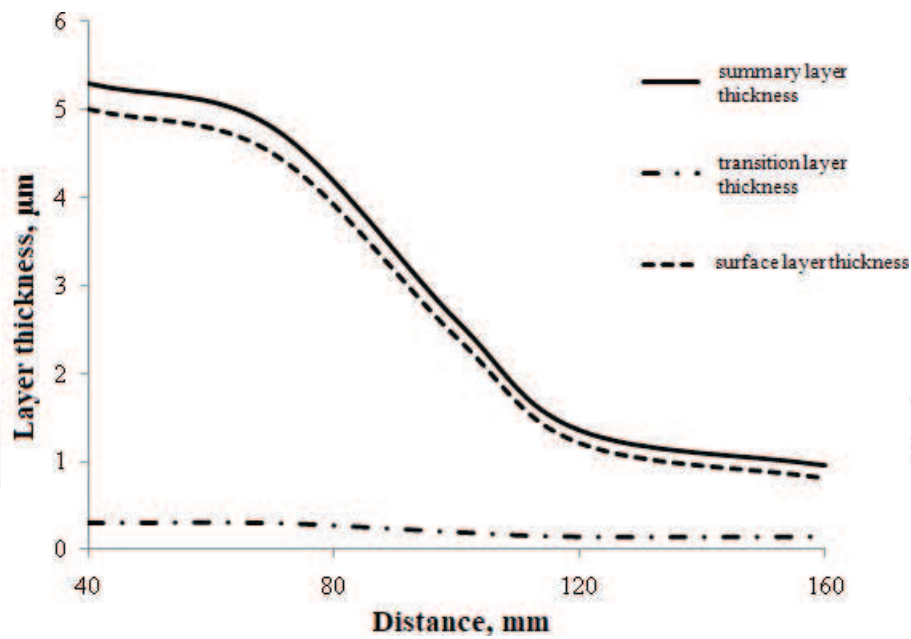


Figure 9.
 Change in the silver surface layers thickness as a function of the distance between the target and the substrate for composite obtained for 30 min.

The morphology of a new surface repeats the substrate state regardless of the sputtering conditions (**Figure 11**). However, at small distances, surface microdefects appear as point depressions (**Figure 12**), recalling effect of high bias voltage and ion implantation [7, 9], which is correlated with a more intense flow of the sprayed material reaching the surface of the substrate, in comparison with larger distances. Formation of layers on the side that is opposite to the sputtered flow was noted. In this case, the structure and patterns of these layers changes are analogous to the straight side, but every 10–15 times thinner (**Figure 13**). This also could be accounted for by a large sputtering distance: when particles that are sputtered travel over large distances, they completely lose additional energy and directed movement, slow down to thermal velocities corresponding to the gas temperature, start to move like any atoms in a gaseous state, and can condense at the opposite side of the substrate upon collision with it [7]; there is also the possibility that sputtered atoms

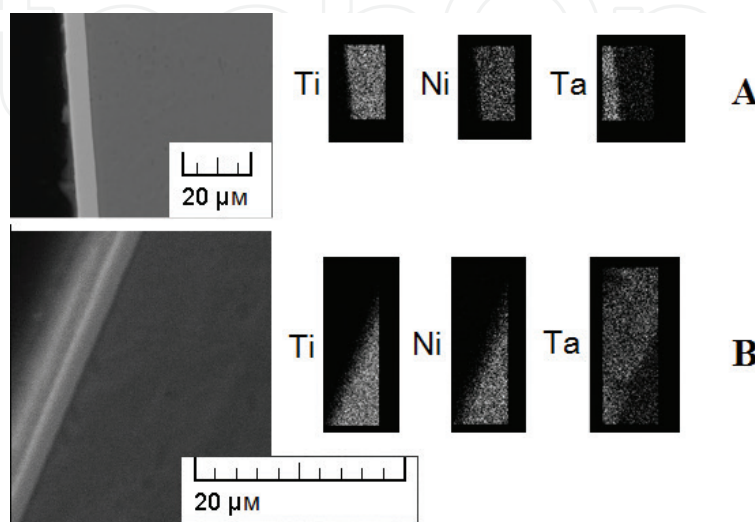


Figure 10.
 Dependence of the thickness of the surface tantalum layer distribution of elements in the structure of composites produced on a nitinol substrate for 120 min at ~865 mA, ~700 V, $U_b \sim 1000$ V, and with PIE on the sputtering distance. The sputtering distance was (a) 100 and (b) 200 mm, while the layer thickness was (a) 6.3 and (b) 3.6 μm.

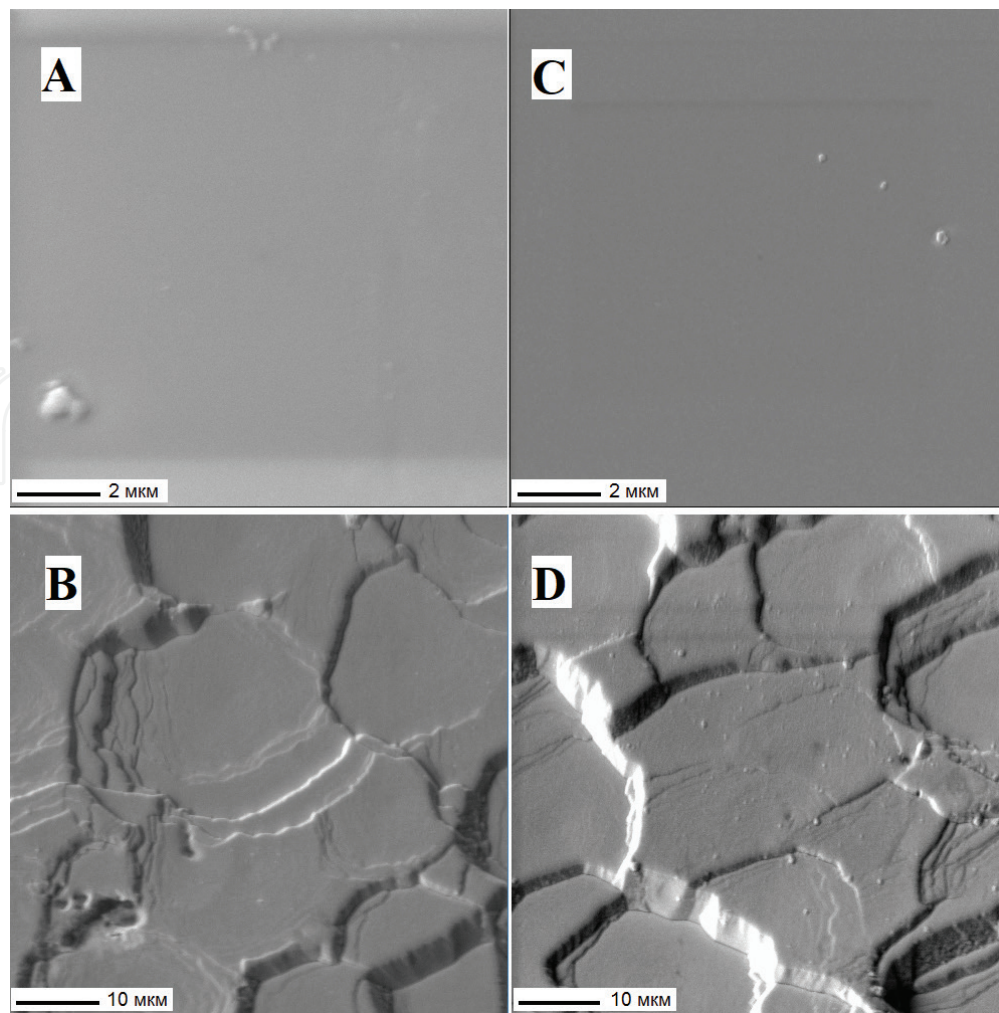


Figure 11. Morphology of the surface of a glass substrate, straight side (a) and opposite side (b), and a silver layer that is formed on it, straight side (c) and opposite side (d), by sputtering for 20 min at a distance of 70 mm.

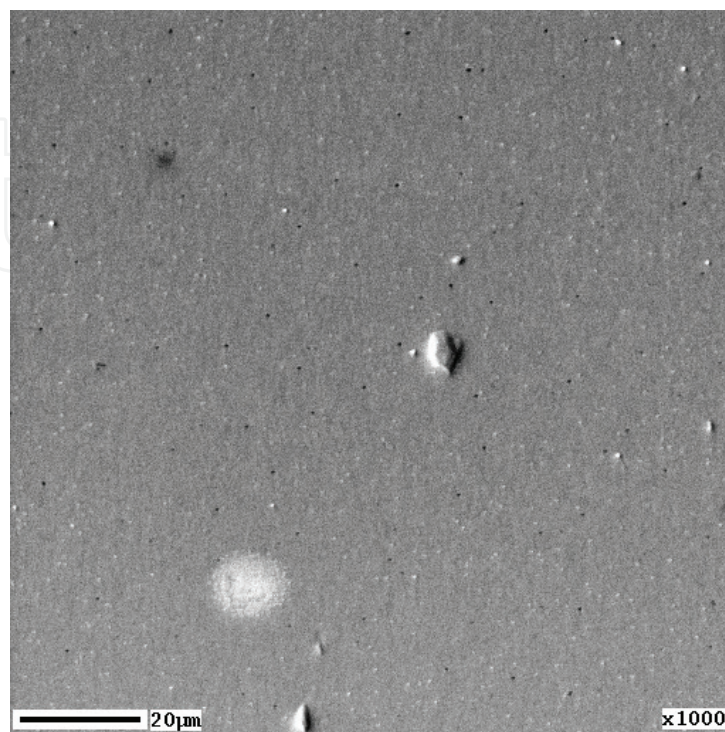


Figure 12. Morphology of the silver surface layer sputtered for 20 min at a distance of 40 mm.

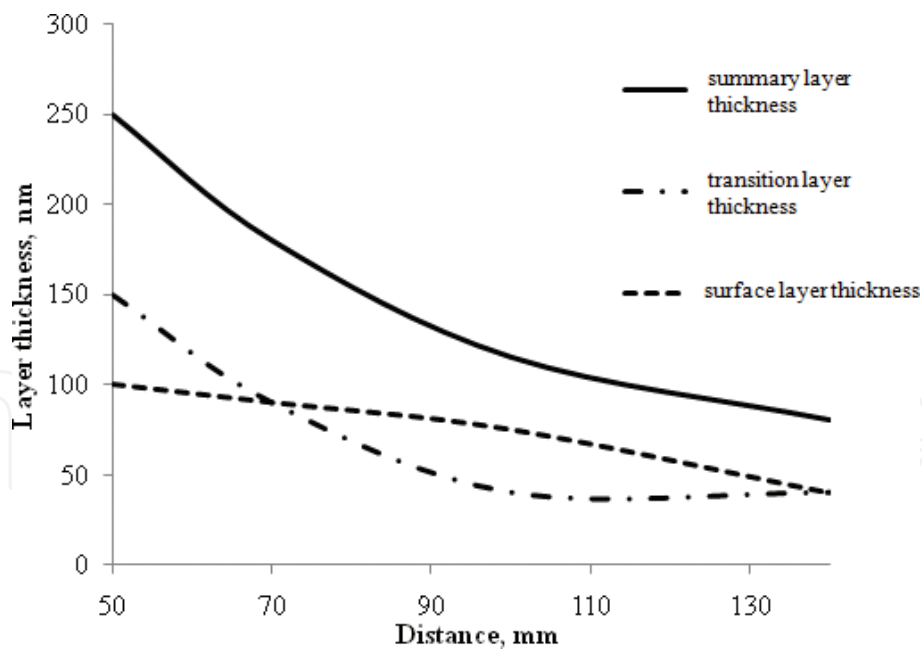


Figure 13. Change in the tantalum surface layers' thickness as a function of the distance between the target and the substrate on the opposite side of the substrate for composite obtained for 30 min at 400 V, 865 mA.

without complete loss of their kinetic energy fall to the opposite side of the substrate as a result of multiple collisions and reflections on atoms of the working gas.

The study of the composites after static breakdown (metal wire) or brittle fracture (glass) showed that their components (the surface layer and the base) were not separated from each other even in the area of failure (**Figure 14**). It was assumed that the presence of the transition layer was the reason for good adhesion between the surface layer and the base. Preliminary ion etching improved adhesion.

The mechanical properties of samples with a working part length of 45 mm were determined under the conditions of static stretching on an Instron 3382 (Instron, USA) universal testing machine with a loading speed of 2 mm/min. The base diameter was used in the calculation of strength properties. Three to five samples were tested per one experimental point. Micro-Vickers hardness measurements determined at loading 1–2 N by the WOLPERT GROUP 401/402 device—MVD (WILSON Instruments, USA) equipped with a light microscope. The conventional yield strength $\sigma_{0.2}$, the ultimate strength σ_u , the relative elongation δ , and microhardness were determined (**Table 1**). Six types of samples were studied: TiNi in the initial state (as-received),

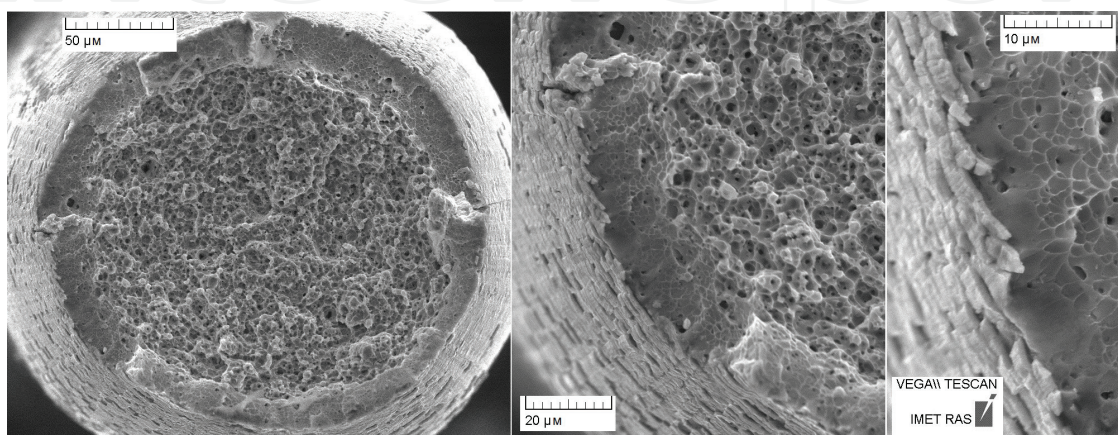


Figure 14. Surface layer in a Ta-nitinol sample on a wire substrate after 80 min of sputtering with rotation at 865 mA, 400 V and distance of 150 mm.

Sample	σ_y , MPa	σ_u , MPa	δ , %	Microhardness, HV
TiNi	547 ± 5	1585 ± 7	47 ± 1	332 ± 3
TiNi after mechanical surface treatment and annealing	641 ± 6	1815 ± 9	54 ± 1	399 ± 3
TiNi after PIE	—	—	—	310 ± 6
Ta@TiNi, 10 min of sputtering	—	—	—	330 ± 4
Ta@TiNi, 30 min of sputtering	652 ± 7	1884 ± 8	55 ± 1	418 ± 4
Ti@TiNi, 30 min of sputtering	648 ± 6	1879 ± 8	55 ± 1	391.4 ± 5

Table 1. Mechanical properties of composites based on nanostructured nitinol with surface layers of tantalum and titanium.

TiNi after polishing and annealing, TiNi after PIE, and composites with Ta and Ti layers. Wires after polishing were annealed at 450°C for 15 min in air as this treatment is needed for end stabilization of the nitinol structure that caused SME and superelasticity and product shaping. Composites were produced at 865 mA, 400 V, a sputtering distance of 150 mm and the conventional sputtering time listed in the **Table 1**.

Results of mechanical stretching tests show positive influence of 1 μm thickness surface layers of Ta and Ti on static properties of a nanostructural alloy, which promotes increase of yield strength and tensile strength by 2–4%. Relative elongation of all samples was of 55%. During preliminary ion etching of the surface of the substrate, bombardment with argon ions is carried out, which facilitates the removal of the surface oxide and the riveted layer with residual surface stresses and defects. Apparently, this explains a slight decrease in the microhardness of the samples immediately after PIE. Two types of composites were studied with a tantalum surface layer obtained for 10 (the main phase β -Ta) and 30 min (the main phase α -Ta formed on the beta phase). The surface of the composite material is distinguished by large microhardness values in comparison with the samples after PIE, since the hardness of both β -Ta and α -Ta is higher than that of nitinol. A thicker surface layer corresponds to higher microhardness values. With respect to the nanostructured substrate, a Ta layer of the order of 1 μm thick, consisting of a mixture of beta and alpha phases, shows an increase in the microhardness by about 26%. In this case, the effect of mechanical surface treatment and annealing on the surface microhardness can be practically neglected in connection with the PIE being carried out. The surface of the titanium layer less significantly affects the microhardness of the nanostructured substrate, but still increases it by 18%.

An object for investigations of corrosion resistance was wires of nanostructural nitinol and composites based on it with tantalum or titanium surface layers. Six types of samples were studied: (1) TiNi in the initial state (as-received), (2) TiNi after annealing, (3) TiNi after polishing, (4) TiNi after polishing and annealing, (5) TiNi-4 with Ta surface layer (Ta-TiNi), and (6) TiNi-4 with Ti surface layer (Ti-TiNi). Composites were produced at 865 mA, 400 V, a sputtering distance of 150 mm, a sputtering time 80 min on the main surface with rotation and 30 min on end faces after PIE. The researched composite materials had layered structure “a surface layer from the deposited substance (thickness ~ 0.9 microns)—the transitional layer containing elements both of the surface layer and of a basis (thickness ~ 0.2 microns)—a basis.”

The material was tested for corrosion resistance under static conditions by dipping into solutions with various acidities because pH in the human body changes from 1 to 9. Neutral 0.9 wt% sodium chloride solution, artificial plasma and saliva, and four standard buffer solutions to reproduce acidic and alkaline media at the given level, and prepared from corresponding standard trimetric substances

(fixanals) made by Merck, were used and listed in **Table 2**. Wire samples with a weight by 32.6 mg (separately from each other) were placed into flasks with 100 mL of the selected solution and aged totally in a dark place for up to 730 days. Sampling from flasks for analysis was after a selected period (7, 14, 30, 60, 90, 180, 360, or 730 days). The initial buffer solutions were used as reference solutions. Analysis was carried out by an ULTIMA 2 sequential atomic emission spectrometry (HORIBA Jobin Yvon, Japan) for using atomic emission spectrometry (AES) with inductively coupled plasma (ICP) for direct simultaneous determination of titanium and nickel in solutions. After immersion, the surface morphology and layer-by-layer composition were also investigated.

In **Figures 15** and **16**, an release of metal ions in model media depending on holding time, material treatment, nature, and temperature of the environment is shown. There are no results about all samples in the alkaline environment, artificial plasma and saliva, and also about TiNi-3, TiNi-4, Ta-TiNi, and Ti-TiNi samples in solutions with acidity 3.56–6.31, since in these cases, dissolution of elements was zero or below a limit of detection for all the time of a research. So, all further results concern only a solution with a pH of 1.68.

In the remained cases, elements' concentration in solutions increases (**Figures 15** and **16**) over time, but leaching of elements in medium considerably slows down. It can be related to sequential processes of the destruction and renewal of the protective film (de- and repassivation) on defect areas [30, 31].

Medium temperature growth insignificantly increases concentration of elements in solution (varies depending on immersion time and metal nature), but at the same time, the gradual inhibition of material dissolution is also observed, and at different temperatures, it occurs almost at the same time (**Figure 15**). It allows to assume that after initial increase in corrosion due to temperature increase in the following, with the surface repassivation, the degree of the material dissolution practically does not depend on temperature.

In solution with Ti-TiNi (**Figure 15a**), titanium concentration is approximately twice more than nickel that is explained by chemical interaction of surface layer material with potassium tetraoxalate [31]. In case of composite material with a tantalum surface layer, Ta concentration was also considered (**Figure 15b**). Insignificant dissolution of material is also observed only in the most acidic environment (most likely on possible defective sites of a surface with an incomplete surface layer that requires separate studying), and concentration of tantalum is much less than of titanium, which, respectively, is less, than of nickel.

pH	Composition
1.68	Potassium tetraoxalate: $\text{KH}_3\text{C}_4\text{O}_8 \times 2\text{H}_2\text{O}$, 0.05 M
3.56	Acid potassium tartrate: $\text{C}_4\text{H}_5\text{O}_6\text{K}$, 0.025 M
4.01	Acid potassium phthalate: $\text{C}_8\text{H}_5\text{O}_4\text{K}$, 0.05 M
6.31	Sodium chloride: NaCl, 0.9 wt. %
9.18	Acid sodium tetraborate: $\text{Na}_2\text{B}_4\text{O}_7 \times 10\text{H}_2\text{O}$, 0.05 M
7.36	Artificial plasma: NaCl (92.3 mM), NaHCO_3 (26.3 mM), K_2HPO_4 (0.9 mM), KCl (2.7 mM), NaH_2PO_4 (0.22 mM), CaCl_2 (2.5 mM), $\text{MgSO}_4 \cdot 7\text{H}_2\text{O}$ (0.82 mM), Na_2SO_4 (1.48 mM), D-glucose $\text{C}_6\text{H}_{12}\text{O}_6$ (5.55 mM) [23, 30, 31]
7.55	Artificial saliva: NaCl (13.34 mM), NaHCO_3 (7.4 mM), K_2HPO_4 (4.4 mM), KCl (10 mM), NaH_2PO_4 (1.2 mM), CaCl_2 (1.4 mM), $\text{MgSO}_4 \cdot 7\text{H}_2\text{O}$ (0.7 mM), Na_2SO_4 (0.13 mM), Na_2S (0.021 mM), carbamide (1 g/l) [23, 30, 31]

Table 2.
 The composition and acidity of modeling solutions used for immersion test.

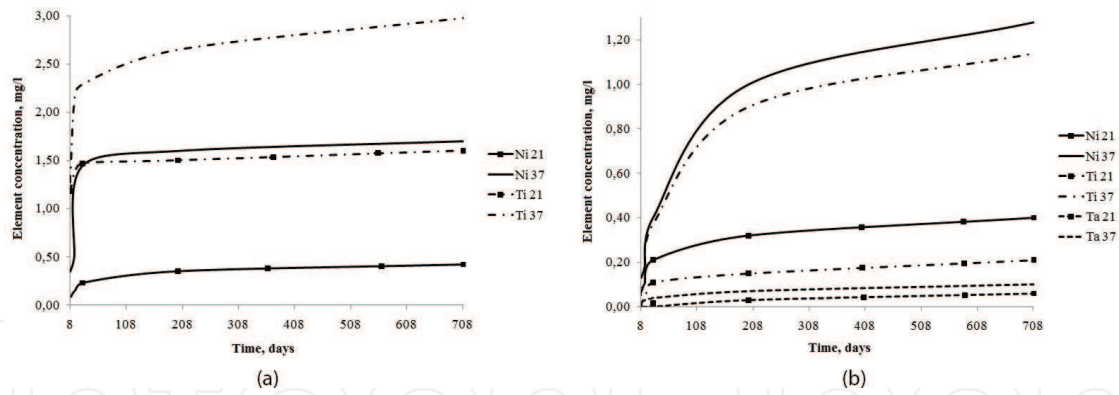


Figure 15. Dependence of concentration of the elements dissolved from TiNi-Ti (a) and TiNi-Ta (b) composites in buffer solution with acidity 1.68 on immersion time of sampling and temperature of solution: the marked curves correspond to temperature of 21°C, curves without tags—37°C.

Depending on material treatment (**Figure 16**), ion release decreases in the following order: TiNi-2 > TiNi-1 > TiNi-4 > TiNi-3 > Ti-TiNi (if to look on nickel concentration) > Ta-TiNi. According to the literature, the thermal treatment at a temperature from 400 to 1000°C, which is required for stabilization of the mechanical properties, always results in a significant worsening of the corrosion resistance [31]. At the same time, the surface treatment, which facilitates the formation of the most perfect and homogeneous passive film, increases the corrosion resistance. Because of chemical interaction of Ti with acid media composite with its surface layer obviously less corrosion resistant than with Ta, but they are both more resistant than nitinol without a protective layer.

Composites Ta-TiNi and Ti-TiNi were also tested for biocompatibility.

The effect on the formation of H₂O₂ in the phosphate buffer (pH 6.8) on heating (37°C) for 200 min in the enhanced chemiluminescence system (luminol–p-iodophenol–peroxidase) [32] was studied. Sputtering of titanium and tantalum decreases the concentration of hydrogen peroxide formed by approximately 40 (6.5 ± 0.5 nM) and 60% (4.5 ± 0.3 nM), respectively, both close to the media concentration 3.2 ± 0.2 nM. By using a fluorescence probe specific to the OH radicals,

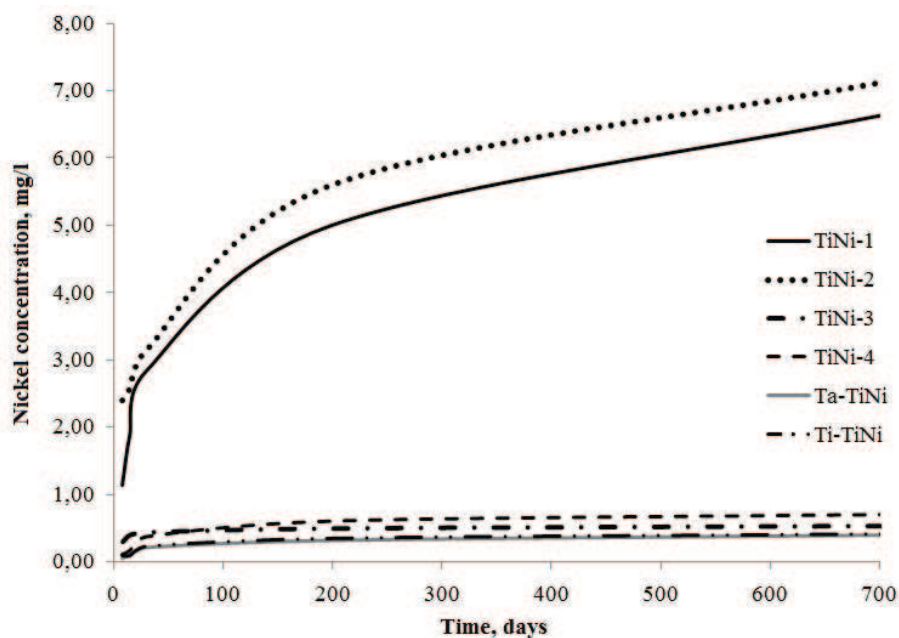


Figure 16. Dependence of nickel concentration in buffer solution with acidity 1.68 at 21°C on immersion time and a sample type.

coumarin-3-carboxylic acid (Aldrich, USA) [33], it was found that all types of barrier coatings decrease the amounts of these radicals formed in a 20 mM phosphate buffer solution (pH 6.8) on heating (80°C) for 2 h. Titanium and tantalum coatings decreased the amount of the hydroxyl radicals by about 70 and 80% (30.9 ± 2.0 and 26.1 ± 1.3 nM), respectively, in comparison with NiTi plates (120.7 ± 4.9 nM). The test systems we used showed that the titanium or tantalum surface composite layers prevent the excessive generation of reactive oxygen species.

The biocompatibility was measured in vitro using standard test systems [34]. Then, the samples were examined under a DM 6000 fluorescence microscope (Leica, Germany). In the case of myofibroblasts from peripheral vessels, the percentages of vital cells for Ta-NiTi and Ti-NiTi were 95 ± 2 and $97 \pm 2\%$, respectively. In the case of the human bone marrow mesenchymal stromal cells (MSC), the percentages of vital cells for Ta-NiTi and Ti-NiTi were 96 ± 3 and $96 \pm 2\%$, respectively. Thus, none of the material surface samples used in the study had a short-term toxic effect on the cells that overgrew these surfaces de novo. The mitotic activity of the cells was assessed considering the mitotic index of the cells in the logarithmic growth phase (the third day after inoculation). The number of mitotic cells was determined by fluorescence microscopy using the vital staining with the Hoechst 33342 fluorescent dye (Sigma, USA). The MI value for the cells growing on the NiTi (reference) surface was 3.1% for the myofibroblast culture and 1.8% for the MSC culture. In the case of Ta-NiTi, the MI was 6.1% for the myofibroblasts and 4.3% for the bone marrow MSC. For the myofibroblasts and MSC cultured on Ti-NiTi, the mitotic indices were 5.8 and 4.7%, respectively. Morphological analysis of the myofibroblasts from peripheral vessels and bone marrow MSC on the surface of materials after 5 days of culturing were performed. Both myofibroblasts and MSC form a merged monolayer on the Ti-NiTi and Ta-NiTi surfaces.

3. Conclusions

Nano- and microdimensional surface layers of α - and β -Ta, Ti, Ag, and Cu on flat and wire NiTi, Cu, Ti, and SiO₂ substrates were created by vacuum magnetron sputtering aimed to investigate regularities of production of layered biomedical composite materials.

It was shown that the thickness and the structure of surface layers were affected by the sputtering distance, time, power, and the bias voltage at the substrate. The presence of the transition layer that contains both substrate and target elements and provides high adhesion of the surface layer to the substrate has been demonstrated. The morphology of a new surface repeats the substrate state regardless of the sputtering conditions.

With increase in deposition time, surface layer thickness does not linearly increase. Irrespective of summary sputtering time, the β phase is formed in the beginning, and at summary, surface layer thickness more than 0.6 μm on it α tantalum is deposited, while temperature remains below 150°C. The optimum bias voltage (500 V) for ion-atomic deposition was determined. It was demonstrated that an increase in power from 50 to 70% enhanced the thickness and uniformity of both the surface and the transition layers without their contamination.

A nonlinear increase in the thickness of the growing surface layers with decreasing sputtering distance under otherwise equal conditions was demonstrated. But the thickness of the transition layer and the dependence of the thickness change as a whole depend on the nature of the sputtered substance. It has been shown that at distances of 40–160 mm, insignificant deposition on the substrate side that is

opposite to the sputtered flow is observed, with the thickness of formed layers also depending on the distance between the target and the substrate.

A slight corrosive dissolution was observed only in a medium with a pH of 1.56 for 2 years of a research. Dissolution in the other media is absent. Concentration of metals increases in solution over time, but the considerable slowdown of a metal ion release in solutions is observed over time. An increase in strength and plasticity in comparison with substrate was attained depending on the nature of the sputtered substance and substrate. Toxicity of samples has not been revealed.

Thus, the growth of a thin surface layer with high corrosion resistance and good biocompatibility by magnetron sputtering allows one to obtain a barrier to nitinol contact with physiological medium, which can withstand loads when nitinol exhibits superelasticity and an SME, with the formation of a transition layer, but no nitinol phase state changing.

Acknowledgements

The authors wish to thank Dyomin K Yu, Mikhailova AB, Gol'dberg MA, Kargin Yu F, and Gudkov SV for their help in sample analysis. The work was partially carried out under state assignment no. 007-00129-18-00 and was supported by the Russian President Program for Young Scientists (MK-4521.2018.8).

Chapter is partially based on the results of earlier published works [35–37], and authors have the permission to re-use it.

Conflict of interest

There is no conflict of interest to declare.

Author details

Elena O. Nasakina*, Mikhail A. Sevostyanov, Alexander S. Baikin,
Sergey V. Konushkin, Konstantin V. Sergienko, Mikhail A. Kaplan, Ilya M. Fedyuk,
Alexander V. Leonov and Alexey G. Kolmakov
A.A. Baikov Institute of Metallurgy and Material Science, Moscow, Russia

*Address all correspondence to: nacakina@mail.ru

IntechOpen

© 2018 The Author(s). Licensee IntechOpen. This chapter is distributed under the terms of the Creative Commons Attribution License (<http://creativecommons.org/licenses/by/3.0>), which permits unrestricted use, distribution, and reproduction in any medium, provided the original work is properly cited. 

References

- [1] Stolin AM, Bazhin PM. Manufacture of multipurpose composite and ceramic materials in the combustion regime and high-temperature deformation (SHS extrusion). *Theoretical Foundations of Chemical Engineering*. 2014;**48**(6):751-763. DOI: 10.1134/S0040579514060104
- [2] Bazhin PM, Stolin AM, Alymov MI. Preparation of nanostructured composite ceramic materials and products under conditions of a combination of combustion and high-temperature deformation (SHS extrusion). *Nanotechnologies in Russia*. 2014;**9**(11-12):583-600. DOI: 10.1134/S1995078014060020
- [3] Maho A, Kanoufi F, Combellas C, Delhalle J, Mekhalif Z. Electrochemical investigation of nitinol/tantalum hybrid surfaces modified by alkylphosphonic self-assembled monolayers. *Electrochimica Acta*. 2014;**116**:78-88. DOI: 10.1016/j.electacta.2013.11.008
- [4] Krivoschapkin PV, Mikhaylov VI, Krivoshapkina EF, Zaikovskii VI, Melgunov MS, Stalugin VV. Mesoporous Fe-alumina films prepared via sol-gel route. *Microporous and Mesoporous Materials*. 2015;**204**:276-281. DOI: 10.1016/j.micromeso.2014.12.001
- [5] Kononova SV, Romashkova KA, Kruchinina EV, Gusarov VV, Potokin IL, Korytkova EN, Maslennikova TP. Polymer-inorganic nanocomposites based on aromatic polyamidoimides effective in the processes of liquids separation. *Russian Journal of General Chemistry*. 2010;**80**(6):1136-1142. DOI: 10.1134/S1070363210060162
- [6] Nasakina EO, Baikin AS, Sevost'yanov MA, Kolmakov AG, Zabolotnyi VT, Solntsev KA. Properties of nanostructured titanium nickelide and composite based on it. *Theoretical Foundations of Chemical Engineering*. 2014;**48**(4):477-486. DOI: 10.1134/S0040579514040071
- [7] Kuz'michev AI. Magnetronnye raspylitel'nye sistemy. Kn. 1. Vvedenie v fiziku i tekhniku magnetronnogo raspyleniya [Magnetron Scattering Systems. Book 1. Introduction into Physics and Technique of Magnetron Scattering]. Kiev: Avers; 2008. 244 p. (Russian)
- [8] Bunshah RF. *Deposition Technologies for Films and Coating*. Park Ridge, New Jersey (USA): Noyes Publications; 1982
- [9] Poate JM, Foti G, Jacobson DC. *Surface Modification and Alloying by Laser, Ion and Electron Beams*. New York: Plenum; 1983
- [10] Dorranean D, Solati E, Hantezadeh M, Ghoranneviss M, Sari A. Effects of low temperature on the characteristics of tantalum thin films. *Vacuum*. 2011;**86**:51-55. DOI: 10.1016/j.vacuum.2011.04.012
- [11] Bernoulli D, Müller U, Schwarzenberger M, Hauert R, Spolenak R. Magnetron sputter deposited tantalum and tantalum nitride thin films: An analysis of phase, hardness and composition. *Thin Solid Films*. 2013;**548**:157-161. DOI: 10.1016/j.tsf.2013.09.055
- [12] Zhou YM, Xie Z, Ma YZ, Xia FJ, Feng SL. Growth and characterization of Ta/Ti bi-layer films on glass and Si (111) substrates by direct current magnetron sputtering. *Applied Surface Science*. 2012;**258**:7314-7321. DOI: 10.1016/j.apsusc.2012.03.176
- [13] Navid AA, Chason E, Hodge AM. Evaluation of stress during and after sputter deposition of Cu and Ta films. *Surface and Coating Technology*.

2010;**205**:2355-2361. DOI: 10.1016/j.surfcoat.2010.09.020

[14] Myers S, Lin J, Martins Souza R, Sproul WD, Moore JJ. The β to α phase transition of tantalum coatings deposited by modulated pulsed power magnetron sputtering. *Surface and Coating Technology*. 2013;**214**:38-45. DOI: 10.1016/j.surfcoat.2012.10.061

[15] Cacucci A, Loffredo S, Potin V, Imhoff L, Martin N. Interdependence of structural and electrical properties in tantalum/tantalum oxide multilayers. *Surface and Coating Technology*. 2013;**227**:38-41. DOI: 10.1016/j.surfcoat.2012.10.064

[16] Navid AA, Hodge AM. Nanostructured alpha and beta tantalum formation—Relationship between plasma parameters and microstructure. *Materials Science and Engineering A*. 2012;**536**:49-56. DOI: 10.1016/j.msea.2011.12.017

[17] Navid AA, Hodge AM. Controllable residual stresses in sputtered nanostructured alpha-tantalum. *Scripta Materialia*. 2010;**63**:867-870. DOI: 10.1016/j.scriptamat.2010.06.037

[18] Zabolotnyi VT. Ionnoe peremeshivanie v tverdykh telakh [Ion Intermixing in Solids]. Moscow: MGIEM (TU); 1997 (Russian)

[19] Bose A, Hartmann M, Henkes H. A novel, self-expanding, nitinol stent in medically refractory intracranial atherosclerotic stenosis. *The Wingspan Study, Stroke*. 2007;**38**:1531-1537. DOI: 10.1161/STROKEAHA.106.477711

[20] Stoeckel D. Nitinol medical devices and implants. *Minimally Invasive Therapy & Allied Technologies*. 2000;**9**:81-88. DOI: 10.3109/13645700009063054

[21] Petrini L, Migliavacca F. Biomedical applications of shape memory alloys. *Journal of Metallurgy*. 2011;**2011**:1-15. DOI: 10.1155/2011/501483

[22] Zabolotnyi VT, Belousov OK, Palii NA, Goncharenko BA, Armaderova EA, Sevost'yanov MA. Materials science aspects of the production, treatment, and properties of titanium nickelide for application in endovascular surgery. *Russian Metallurgy*. 2011;**5**:437-448. DOI: 10.1134/S003602951105017X

[23] In: Ebrahim F, editor. *Shape Memory Alloys—Fundamentals and Applications*. Croatia, Rijeka: InTech d.o.o.; 2017. 134 p. Chapter 4. pp. 81-104. DOI: 10.5772/intechopen.69238

[24] Choi J, Bogdanski D, Köller M, Esenwein SA, Müller D, Muhr G, Epple M. Calcium phosphate coating of nickel–titanium shape-memory alloys. Coating procedure and adherence of leukocytes and platelets. *Biomaterials*. 2003;**24**:3689-3696. DOI: 10.1016/S0142-9612(03)00241-2

[25] Tan L, Dodd RA, Crone WC. Corrosion and wear-corrosion behavior of NiTi modified by plasma source ion implantation. *Biomaterials*. 2003;**24**:3931-3939. DOI: 10.1016/S0142-9612(03)00271-0

[26] Chen Y-H, Hsu C-C, He J-L. Antibacterial silver coating on poly (ethylene terephthalate) fabric by using high power impulse magnetron sputtering. *Surface and Coating Technology*. 2013;**232**:868-875. DOI: 10.1016/j.surfcoat.2013.06.115

[27] Cheng Y, Cai W, Li HT, Zheng YF. Surface modification of NiTi alloy with tantalum to improve its biocompatibility and radiopacity. *Journal of Materials Science*. 2006;**41**:4961-4964. DOI: 10.1007/s10853-006-0096-6

- [28] Zhang M, Yang B, Chu J, Nieh TG. Hardness enhancement in nanocrystalline tantalum thin films. *Scripta Materialia*. 2006;**54**:1227-1230. DOI: 10.1016/j.scriptamat.2005.12.027
- [29] Zhou YM, Xie Z, Xiao HN, Hu PF, He J. Effects of deposition parameters on tantalum films deposited by direct current magnetron sputtering. *Journal of Vacuum Science and Technology A*. 2009;**83**:286-291. DOI: 10.1116/1.304614
- [30] Nasakina EO, Sevostyanov MA, Golberg MA, et al. Long term corrosion tests of nanostructural nitinol of (55.91 wt% Ni, 44.03 wt% Ti) composition under static conditions: Composition and structure before and after corrosion. *Inorganic Materials: Applied Research*. 2015;**6**(1):53-58. DOI: 10.1134/S2075113315010104
- [31] Nasakina EO, Sevostyanov MA, Golberg MA, et al. Long term corrosion tests of nanostructural nitinol of (55.91 wt% Ni, 44.03 wt% Ti) composition under static conditions: ion release. *Inorganic Materials: Applied Research*. 2015;**6**(1):59-66. DOI: 10.1134/S2075113315010116
- [32] Shtarkman IN, Gudkov SV, Chernikov AV, Bruskov VI. Effect of amino acids on X-ray-induced hydrogen peroxide and hydroxyl radical formation in water and 8-oxoguanine in DNA. *Biochemistry (Moscow)*. 2008;**73**:470-478. DOI: 10.1134/S0006297908040135
- [33] Bruskov VI, Karp OE, Garmash SA, et al. Free Radical Research. 2012;**46**:1280-1290. DOI: 10.3109/10715762.2012.709316
- [34] Garmash SA, Smirnova VS, Karp OE, et al. Pro-oxidative, genotoxic and cytotoxic properties of uranyl ions. *Journal of Environmental Radioactivity*. 2014;**127**:163-170. DOI: 10.1016/j.jenvrad.2012.12.009
- [35] Nasakina EO, Sevost'yanov MA, Mikhailova AB, Gol'dberg MA, Demin KY, Kolmakov AG, Zabolotnyi VT. Preparation of a nanostructured shape memory composite material for biomedical applications. *Inorganic Materials*. 2015;**51**(4):400-404
- [36] Nasakina EO, Sevostyanov MA, Mikhaylova AB, Baikin AS, Sergienko KV, Leonov AV, Kolmakov AG. Formation of alpha and beta tantalum at the variation of magnetron sputtering conditions. *IOP Conference Series: Materials Science and Engineering*. 2016;**110**:012042
- [37] Nasakina EO, Seregin AV, Baikin AS, Kaplan MA, Konushkin SV, Sergiyenko KV, et al. Formation of biocompatible surface layers depending on the sputtering distance. *IOP Conference Series: Journal of Physics: Conference Series*. 2017;**857**:012032